# Evaporation and Diffusion of Mn in Inert Systems

Håkon Aleksander Hartvedt Olsen, Stefan Andersson, and Gabriella Tranell

**Abstract**

This research is aimed to improve our knowledge on the dust formation and clustering in the ferroalloy industry. Specifically, this paper focuses on the evaporation of manganese metal, and how different parameters influence the evaporation rate. Experiments were done with pure manganese metal heated to between 1400 and 1700°C in a pure argon atmosphere, where the change in weight was measured to calculate the loss of manganese over time. A mathematical model was constructed to link theoretical values to the results from the experiments. The high control over the system parameters allowed for the validation, rejection or creation of values and theories used in the model.

**Keywords**

Manganese, Evaporation, Diffusion, CFD

## 1 Introduction

Airborne particulate matters, originating from various sources in the metallurgical industry are not only a concern in terms of workers health, but the fumes from industrial plants also contribute to the so-called fugitive emissions which may be harmful to the local, urban communities as well as the environment at large.

Håkon Aleksander Hartvedt Olsen, PhD Candidate
Department of Materials Science and Engineering, Norwegian University of Science and Technology, Alfred Getz vei 2, NO-7491, Trondheim, Norway, e-mail: hakon.a.h.olsen@ntnu.no

Stefan Andersson, Research scientist
SINTEF Materials and Chemistry, P.O. Box 4760 Torgarden, NO-7465 Trondheim, Norwaye-mail: Stefan.Andersson@sintef.no

Gabriella Tranell, Professor
Department of Materials Science and Engineering, Norwegian University of Science and Technology, Alfred Getz vei 2, NO-7491, Trondheim, Norway, e-mail: Gabriella.tranell@ntnu.no

The aerosols produced in most metallurgical processes may be harmful if inhaled and exposure to high levels of particles has been linked to cancer, pneumonia, chronic obstructive pulmonary disease (COPD) and other respiratory and cardiovascular syndromes [1][2][3][4][5]. Inhalation of certain manganese (Mn) compounds has also been linked to inflammation and neuropsychological disturbances [6][7][8].

Characteristic properties of the particles, especially particle size and chemical composition, may influence their impact on human health. It is now well known that ultrafine particles (nanoparticles, particles <100 nm) have a much greater surface area and different physic-chemical characteristics [9][10] compared to their larger counterparts. They may therefore be more reactive, behave differently in the respiratory system, and give rise to increased biological responses [11].

As the chemical composition and morphology (particle shape) of particles originating from different ferroalloy industries and processes vary greatly, it is important to understand the mechanisms of which dusts are generated and how the characteristic properties of the particles depend on process parameters. With such knowledge, primary dust generation may be partially controlled.

An important and not yet thoroughly studied part of the dust formation from liquid manganese alloys such as ferromanganese (FeMn) and silicomanganese (SiMn) is the evaporation and gas-phase diffusion of manganese. In contrast to silicon, which has a very low vapor pressure and will mostly react with oxygen to form dust, manganese evaporates noticeably at temperatures close to the melting point. With silicomanganese, this leads to possible reactions between silicon oxides and manganese fumes, but can also cause a competition for oxygen close to the surface where if no oxygen reaches the surface, one might get no silicon in the dust at all. [12] Because of these reasons, the experimental study and subsequent modelling of evaporation rates of Mn is important.

## 2 Model development

In the production process for ferroalloys such as ferromanganese and silicomanganese, the produced melt is in contact with air during several steps of the process. Most notably during tapping, refining and casting, the melt is exposed to air without a protective slag layer over an extended duration. During this time, there are two possible reactions for each metal in the

alloy, Evaporation and oxidation, which may be summed as shown in equation 1 and 2.

$$Me(l) \Rightarrow Me(g) \quad (1)$$

$$Me(l) + xO_2(g) \Rightarrow MeO_{2x}(s,l) \quad (2)$$

Both reactions are thermodynamically driven towards equilibrium, and the distance from equilibrium is the driving force of the mass flux. This work purely studies reaction 1. for pure manganese, and the equilibrium partial pressure for this reaction is defined as shown in equation 3.

$$p_{eq} = \frac{1}{exp(^{-\Delta G}/_{R*T})} \quad (3)$$

Where R is the gas constant, T is the temperature in Kelvin, and $\Delta G$ is the change in Gibbs free energy. The Gibbs free energy for each side of the equation is calculated as shown in equation 4.

$$G = H - TS \quad (4)$$

Where S is the entropy and H is the enthalpy of formation. The flux from evaporation at the surface can then be defined as shown in equation 5,

$$Flux_{evaporation} = (p_{eq} - p) * \sqrt{\frac{Mm}{N_A*2*\pi*k_B*T}} \quad (5)$$

Here, $N_A$ is Avogadro's number, $k_B$ is Boltzmann's constant, and Mm is the molar mass of Mn. For diffusion, the flux can be defined by equation 6,

$$Flux_{diffusion} = D * \frac{(n_{eq} - n_{bulk})}{DiffZ} * \frac{Mm}{N_A} \quad (6)$$

Where DiffZ is the diffusion layer thickness defined by equation 7 [13], D is the diffusion coefficient, and n is the molar concentration of Mn(g) for equilibrium and bulk gas respectively.

$$DiffZ = \frac{L*4.52}{Re^{1/2}*Sc^{1/3}} \quad (7)$$

Reynold's number and Schmidt's number are defined by equation 8 and 9 respectively. L is here defined as the radius of the crucible, $\nu$ is the viscosity, v is the bulk flow velocity, D is the diffusion coefficient and $\rho$ is the density of the gas.

$$Re \quad \frac{v*L*\rho}{\nu} \quad (8)$$

$$Sc = \frac{\nu}{D*\rho} \quad (9)$$

In order to model the evaporation and diffusion kinetically, diffusion coefficients for Mn and Ar gas as well as a Mn-Ar gas mixture were derived from Chapman-Enskog kinetic theory [14] based on Lennard-Jones parameters for Ar-Ar and a Morse potential used to describe the Mn-Mn and Mn-Ar interactions. The Ar-Ar parameters were taken from the literature [14] whereas the Mn-Ar and Mn-Mn interaction potentials were evaluated by high-level quantum chemical calculations. Coupled cluster with single and double excitations with a perturbative treatment of triple excitations [CCSD(T)][15] calculations were applied to Mn-Mn and Mn-Ar pair interactions at a range of separation distances (3-7 Å) using the CFOUR program package [16]. These results were subsequently fitted to Morse potentials, respectively, since the Lennard-Jones potential was found not to reproduce the calculated interaction energy curves well enough. Expressions and values of collision integrals for calculating diffusion coefficients for the two types of potential were taken from literature [14,17].

The model for the evaporation was created in two parts: One that calculated the flux of vaporization using thermodynamic and kinetic data, and one that calculated the diffusion flux from flow conditions and kinetic theory. For each temperature and flow rate investigated experimentally (see section 3), the gas velocity over the metal surface was calculated using a Comsol model. The model uses finite element analysis, assuming steady state and incompressible flow, and using laminar flow conditions as the calculated Reynold's number for the relevant area is less than 100. The mesh used is shown in Figure 1, it can be noted that a finer mesh is used near the metal surface. For the surfaces, no slip is the assumed boundary condition, and for each element, a form of the Navier-Stokes equation and the continuity equation are solved. The exact equations solved are shown in equation (10) and (11) [18].

$$\rho(\boldsymbol{u} \cdot \nabla)\boldsymbol{u} = \nabla[-\mathrm{p}\mathbf{I} + \mu(\nabla\mathbf{u} + (\nabla\mathbf{u})^T)] + \boldsymbol{F} \quad (10)$$

$$\rho\nabla \cdot (\mathbf{u}) = 0 \quad (11)$$

Where **u** is the velocity field, $\rho$ is the density, μ is the dynamic viscosity, p is the pressure, **F** is the external force, and **I** is the identity matrix. The flow pattern for one experiment is shown in Figure 2, with Figure 3 showing a more detailed image of the flow pattern close to the metal surface.

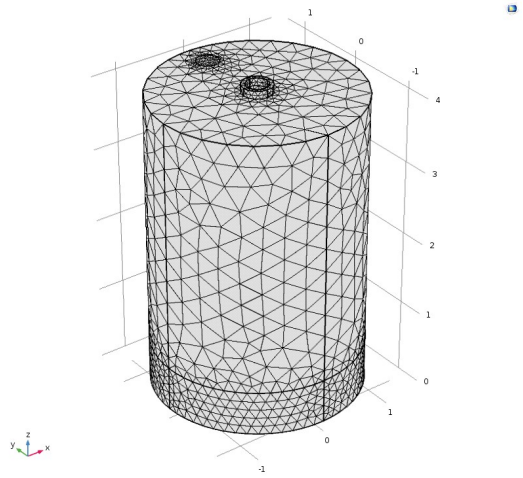

*Figure 1: The mesh used in the comsol model. It has a total of 36587 domain elements, 4286 boundary elements, and 395 edge elements.*

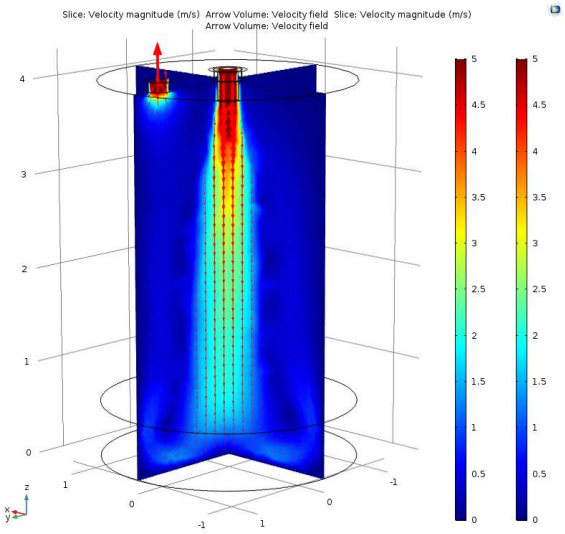


*Figure 2: Flow conditions inside crucible, model made using Comsol software. Conditions assumed: laminar flow, no slip boundaries, incompressible flow, steady state. This image was from an experiment with T = 1550 °C and 0.5 l/min flow rate.*

The thermodynamic data used in the model was taken from NIST-JANAF Thermochemical Tables [19], where values for gases below boiling temperature were extrapolated from the data given. The extrapolated data was found not to deviate much at 1400 °C. Other parameters used in the model are listed in table 1.

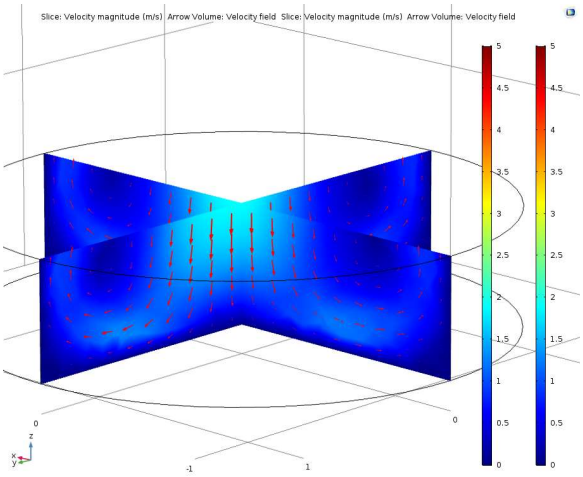


*Figure 3: Flow conditions near the metal surface, model made using Comsol software. Conditions assumed: laminar flow, no slip boundaries, incompressible flow, steady state. This image was from an experiment with T = 1550 °C and 0.5 l/min flow rate.*

*Table 1: Parameters used in the model.*

| **Parameter** | **Value** |
|---|---|
| L | 0.0135 m |
| $Mm_{Mn}$ | 0.054938 kg/mol |
| $\nu$ | 8.42-7.87 * $10^{-5}$ Pa*s |
| D | 2.93-3.97 *$10^{-4}$ $m^2/s$ |
| $\rho$ | 0.246-0.290 $kg/m^3$ |

These two parts are both dependent on the partial pressure of Mn(g) just above the surface of the metal. We know however, that under stable conditions, there is a constant flux of vapour from the surface to the bulk phase, which means the flux from metal to diffusion layer and through the layer to the bulk must be equal. Using the solver function in Excel, the partial pressure at which these two fluxes are equal can then be found, which gives the total flux through the system.

## 3 Experiments

The apparatus used for the experiments was a graphite tube furnace, the design which is sketched in Figure 2. The inside of the furnace was kept in an 6N argon atmosphere of around 1.3 bar to avoid oxidation. Inside the graphite tube, an alumina crucible with height 40mm and diameter 27mm was used as the container for the experiments. The crucible was fitted with a lid to further limit contamination from the

surrounding atmosphere, and an alumina paste was used to seal the lid. An alumina tube with inner diameter of 3mm was inserted into a hole in the center of the lid, through which argon was blown into the crucible. Another hole in the lid with diameter 3mm was the only outlet in the system. Figure 3 shows a crucible after a finished experiment, without the alumina tube.

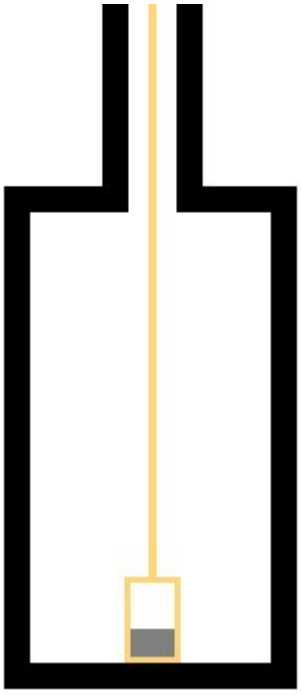

*Figure 4: Sketch of the experimental setup. An outer tube of graphite with an inner alumina crucible and tube connected to an argon source. The atmosphere inside the tube was purged with argon before and during the experiments, and argon was blown at different rates through the tube in each experiment.*

*Figure 5: Alumina crucible after finished experiment. The middle hole was used for the alumina tube, while the smaller hole was used as the outlet for the gas and vapor.*

The crucible was filled with 15 (+/- 0.5) grams of 99.9% Mn chips. The chips had a slightly tarnished, oxidized surface before the experiments and as such, there was a small amount of oxide present in the experiments. However, as a first approach, this was assumed not to affect the evaporation rate. Each sample was pre-treated at 150 °C for 30 minutes to remove any humidity from the sample and the sealing paste, and the crucible set-up was weighted before and after pre-treatment as well as after the experiment. Longer pre-treatment time or higher temperatures were found not to produce any further weight loss in the sample.

The sample was inserted into the furnace, which was then vacuumed to between 80 and 200 mTorr before it was purged with argon and kept at around 1.3 bar. After purging, the chamber was heated to the desired temperature over 30 minutes and held at that temperature for further 60 minutes before being cooled. During the entire heating, holding and cooling period, argon was inserted through the alumina tube at a constant flowrate. The different temperatures and flowrates for each experiment are shown in Table 2.

*Table 2: Flow rates, temperatures, holding times, and Sample contents for the experiments*

| Exp # | Ar flow rate (l/min) | Temp (°C) | Holding time (min) | Sample content |
|---|---|---|---|---|
| 10 | 0.0 | 1400 | 60 | 100% Mn |
| 5 | 0.5 | 1400 | 60 | 100% Mn |
| 7 | 1.0 | 1400 | 60 | 100% Mn |
| 2 | 0.0 | 1550 | 60 | 100% Mn |
| 12 | 0.25 | 1550 | 60 | 100% Mn |
| 3 | 0.5 | 1550 | 60 | 100% Mn |
| 6 | 0.5 | 1550 | 60 | 100% Mn |
| 1 | 1.0 | 1550 | 60 | 100% Mn |
| 4 | 1.0 | 1550 | 60 | 100% Mn |
| 8 | 0.0 | 1700 | 60 | 100% Mn |
| 11 | 0.5 | 1700 | 60 | 100% Mn |
| 9 | 1.0 | 1700 | 60 | 100% Mn |
| 13 | 1.0 | 1700 | 60 | 100% Mn |

After cooling, the crucible weight was again measured and the mass loss calculated. As the only reaction happening was evaporation of Mn, the flux of Mn out of the system could be calculated for each experiment.

## 4 Results

The measured weight losses for each experiment are shown in Table 3 together with the calculated mass flux and the parameters. Figure 4 show the mass loss as a function of the flow rate with linear trend lines for each temperature.

*Table 3: Experimental results: Total mass loss and flux for each set of parameters.*

| Exp # | Ar flow rate (l/min) | Temp (°C) | Loss (g) | Flux ($g/m^2s$) |
|---|---|---|---|---|
| 10 | 0.0 | 1400 | -0.11 | -0.07 |
| 5 | 0.5 | 1400 | 0.40 | 0.25 |
| 7 | 1.0 | 1400 | 1.00 | 0.61 |
| 2 | 0.0 | 1550 | 0.07 | 0.04 |
| 12 | 0.25 | 1550 | 0.78 | 0.48 |
| 3 | 0.5 | 1550 | 1.66 | 1.02 |
| 6 | 0.5 | 1550 | 1.63 | 1.00 |
| 1 | 1.0 | 1550 | 3.67 | 2.25 |
| 4 | 1.0 | 1550 | 3.18 | 1.95 |
| 8 | 0.0 | 1700 | 0.29 | 0.18 |
| 11 | 0.5 | 1700 | 7.75 | 4.76 |
| 9 | 1.0 | 1700 | 11.24 | 6.90 |
| 13 | 1.0 | 1700 | 10.3 | 6.32 |

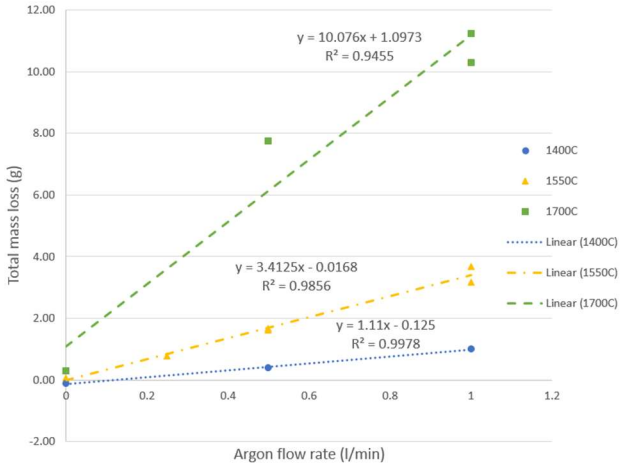


*Figure 6: Total mass loss in grams over the flow rate of argon in l/min. Linear trend lines are given for each temperature.*

## 5. Discussion

The crucible from experiment 10 (1400°, no Ar flow) has increased in weight by a very small amount. A potential reason for this might be a small amount of oxygen, supplied either from the ppm concentration in the Ar, the alumina crucible or from the tarnished starting Mn-chip surface reacting with the metal to form heavier oxides. The amount would not be very high however, and it is assumed that there has been practically no evaporation of manganese in this experiment.

The two experiments at 1700 °C and with 1 l/min flow rate were found to have very little metal left at the end of the experiment. This would likely cause a lower rate of evaporation during the later stages of the experiment as the surface area would be smaller. This would also explain why there is not the same linearity for the 1700 °C experiments as for the lower temperatures. Figure 5 shows the inside of crucible #13, where the metal content has been reduced to the point where it no longer covers the full area of the crucible.

*Figure 7: Crucible from experiment #13, 1700 °C and 1 l/min flow rate. The surface area of the metal is clearly reduced due to excessive evaporation.*

The model does show the same tendency to taper off at higher flow rates, but not to the same degree as in the experiments.

Data from the experiments can be compared with the model, which was used to generate data points for the same parameters as the experiments. These values are shown in Table 3, and plotted in Figure 6.

*Table 3: Modelling results: Total mass loss for a choice set of parameters.*

| Ar flow rate (l/min) | Temp (°C) | Loss (g) |
|---|---|---|
| 0.25 | 1400 | 0.06 |
| 0.5 | 1400 | 0.08 |
| 1.0 | 1400 | 0.12 |
| 0.25 | 1550 | 0.36 |
| 0.5 | 1550 | 0.50 |
| 1.0 | 1550 | 0.71 |
| 0.25 | 1700 | 1.55 |
| 0.5 | 1700 | 2.20 |
| 1.0 | 1700 | 3.11 |

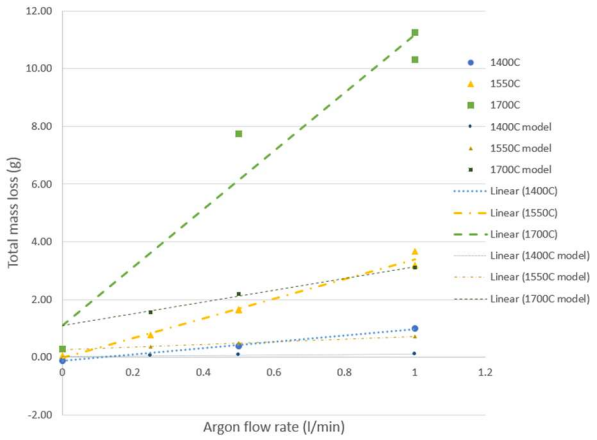


*Figure 8: Mass loss in grams over the flow rate in l/min. Experimental and modelled values.*

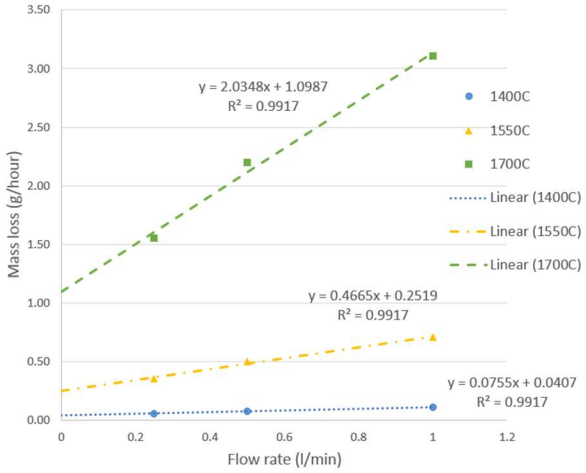


*Figure 9: Modelled mass loss in grams/hour over the flow rate in l/minfrom the model.*

The mass loss calculated with the model are around one fourth of the experimental values for all parameters. For comparison, Figure 7 shows both data sets together.

The curves are similar, but the model has evaporation rates that are about a fourth of the experimental values. Figure 8 shows both data sets together, but with the values from the model multiplied by 4 to show the similarities in the curves.

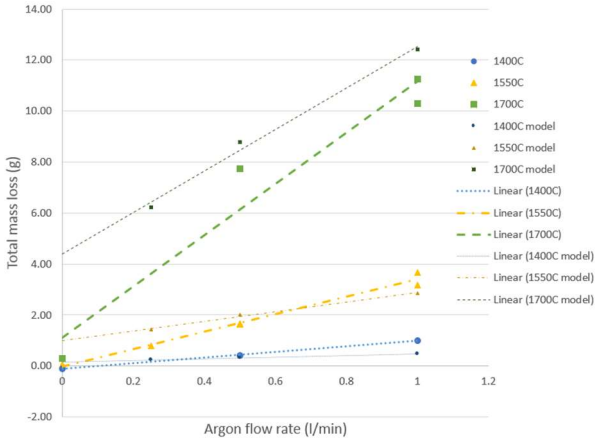


*Figure 10: Mass loss in grams over the flow rate in l/min. Experimental and modelled values. Values from model are multiplied by 4.*

## 6. Conclusions

In order to better understand the kinetics of fume/dust formation in the Mn-ferroalloys production industries, experiments investigating the evaporation rate and diffusion of Mn in an argon atmosphere at different temperatures and flow conditions, have been carried out. The results were compared to values calculated using a mathematical model of the same system. There was a mismatch in the results between model and experiments on the scale of factor 4, but the trends shown were very similar. Possible uncertainties in the model include the diffusion coefficient, enthalpy and entropy at lower temperatures, approximation of Reynolds number, and the gas velocities from the Comsol model.

There are also uncertainties in the experimental work, which could have influenced the experimentally obtained results. The evaporation during heating and cooling might have been measurably large, as there is up to fifteen minutes of time where the temperature is above the melting point during heating and cooling. The flux would in that time probably lie between the values for our experiments. The thin layer of oxide

might have slowed the evaporation process, and the temperature profile might be inaccurate as there is a delay between the outside of the tube where the furnace measures temperature, and the inside of the crucible.

The data from the experiments can be further used when modelling the dust formation in more complex systems where Mn evaporation is just a part of the whole. If improved, the model can also be expanded to take further reactions into account.

## 7. Further work

This work is the beginning of a larger study, and there is much work still to be done. Following is a list of planned work in the continuation of the project:

- Perform experiments where the temperature is measured inside the crucible to find temperature delay.
- Perform experiment without holding time to measure mass loss during heating and cooling.
- Etch the Mn before the experiment to remove any oxides.
- Use a crucible that doesn't contain oxides.
- Perform experiments with 0.25 l/min flow rate for 1400 and 1700°C.
- Review assumptions and uncertainties in the model, and then improve on it.
- Continue the experiments and model work with manganese and iron alloys, as well as including oxygen in the gas.

## References


[1] Johnsen et al. (2008) International Archives of Occupational and Environmental Health 81 p.451-459

[2] Johnsen H L (2009) Ph.D. -thesis. University of Oslo, Fakultetsdivisjon Akershus universitetssykehus

[3] Hobbesland et al. (1997) Scandinavian Journal of Work, Environment and Health 23 5 p. 334-341

[4] Søyseth et al. (2011) American Journal of Industrial Medicine 54 9 p. 707-713

[5] Gibbs et al. (2014) Journal of Occupational and Environmental Medicine 56 7 p. 739-764

[6] Bast-Pettersen et al. (2004) International Archives of Occupational and Environmental Health 77p.277-287

[7] Luccini et al. (2009) Neuromolecular Medicine 11 p.311-321

[8] Racette et al. (2012) Neurotoxicology 33 4 p. 881-886

[9] Monteiller et al. (2007) Occupational and Environmental Medicine 64 p. 609-615

[10] Obersdörster. (2001) International Archives of Occupational and Environmental Health 74 p. 1-8

[11] Schmid et al. (2009) Biomarkers, 14 S1 p. 67-73

[12] Ma Y, Kero I, Tranell G. (2017) Fume Formation from Oxidation of Liquid SiMn Alloy. Oxidation of Metals.

[13] Bakken J A, Lobo S, Kolbeinsen L (2009) Compendium Fluid Flow and Heat Transfer Advanced Course, NTNU.

[14] Bird R B, Stewart W E, Lightfoot E N (2007) Transport Phenomena, Wiley, New York, NY.

[15] Stanton J F, Gauss J, Harding M E, Szalay P G, Auer A A, Bartlett R J, Benedikt U, Berger C, Bernholdt D E, Bomble Y J, et al. (2015) CFOUR, Coupled-Cluster techniques for Computational Chemistry, 2015. For the current version, see http://www.cfour.de.

[16] Bartlett R J, Musial M (2007) Rev. Mod. Phys. 79 p. 291-352

[17] Smith F J, Munn R J (1964) J. Chem. Phys. 41, 3560 – 3568.

[18] Comsol Multiphysics http://www.comsol.com/ comsol-multiphysics. Accessed: 2017-09-06.

[19] Chase M W, Jr. (1998) NIST-JANAF Themochemical Tables, Fourth Edition, J. Phys. Chem. Ref. Data, Monograph 9, 1998, 1-1951.